



INSTITUTE OF MICROELECTRONICS

NSSC2 - EXERCISE 1

Group 9

Member:

Christian GOLLMANN, 01435044

Peter HOLZNER, 01426733

Alexander LEITNER, 01525882

Submission: May 29, 2020

Contents

| | | |
|---|--------------|---|
| 1 | Exercise 1.1 | 1 |
| 2 | Exercise 1.2 | 3 |
| 3 | Exercise 1.3 | 4 |
| 4 | Exercise 1.4 | 5 |
| 5 | Exercise 2.1 | 6 |

1 Exercise 1.1

For Exercise 1.1 we use the following explicit finite difference approach, which is 2nd order accurate in space and 1st order accurate in time:

$$C_i^{n+1} = C_i^n + \frac{\Delta t}{\Delta x^2} \cdot (C_{i-1}^n - 2C_i^n + C_{i+1}^n) = C_i^n + s \cdot (C_{i-1}^n - 2C_i^n + C_{i+1}^n) \quad (1)$$

The update formula above is only applied to all interior points ($x \in (0, h)$) while the boundary values at the left ($x=0$) and right ($x=h$) end are treated separately, according to the boundary condition. Dirichlet boundaries are kept equal to the prescribed condition, e.g. the value for C_0^{n+1} is always kept equal to $C_0^n = 1$ (inhomogenous Dirichlet BC). In order to incorporate Neumann boundary conditions, e.g. the homogenous Neumann boundary condition at $x = h$, we look at the Central discretization in space with respect to figure 1:

$$\begin{aligned} \left[\frac{\delta f}{\delta x} \right]_i &\simeq \frac{f_{i+1} - f_{i-1}}{2\Delta x} \\ \left[\frac{\delta C}{\delta x} \right]_{x=end} &\simeq \frac{C_{end+1} - C_{end-1}}{2\Delta x} = 0 \quad (2) \\ \Rightarrow C_{end+1} &= C_{end-1} \end{aligned}$$

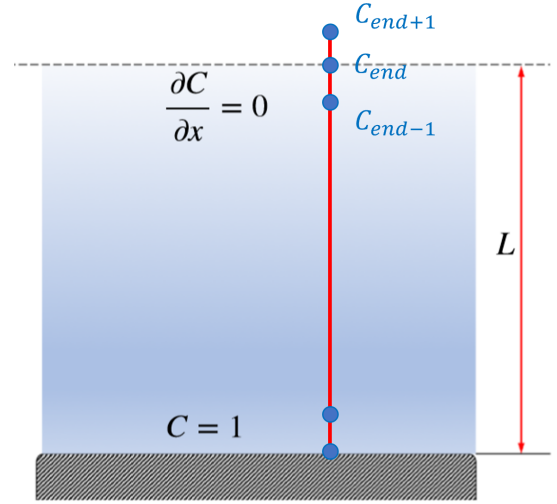


Figure 1: Neumann BC at $x = h$

The findings of equation 2 we plug in equation 1 and end up with equation 3 for C_{end} :

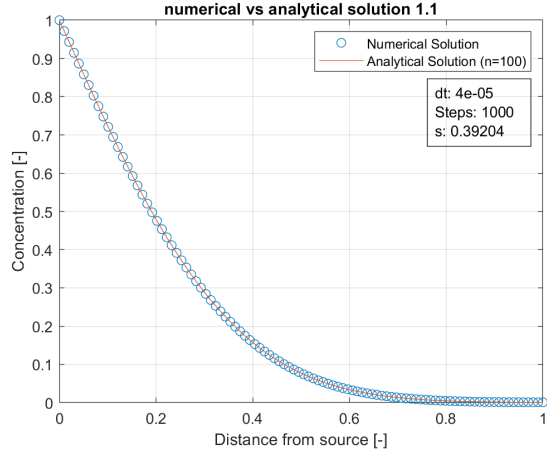
$$C_{end}^{n+1} = C_{end}^n + \frac{\Delta t}{\Delta x^2} \cdot (2C_{end-1}^n - 2C_{end}^n) = C_{end}^n + 2s \cdot (C_{end-1}^n - C_{end}^n) \quad (3)$$

We then let the simulation run with different values for s . In the case where $s \leq 0.5$, we see that the numerical solution is unconditionally stable. For $s > 0.5$, the numerical solution starts to drift off as expected.

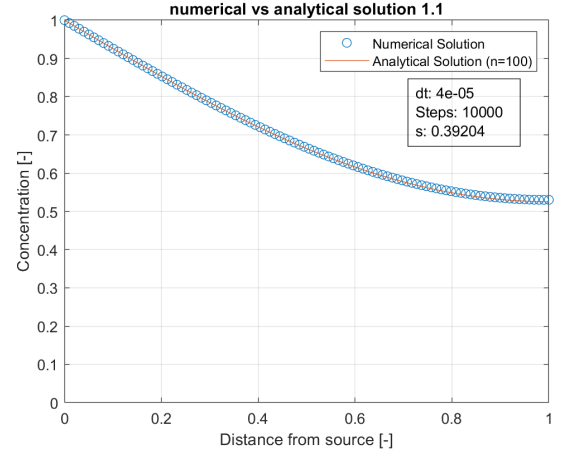
In this and all further elaborations we work with an already dimensionless formulation of the equation and therefore do not take the D into account and let h fixed with 1. If we wanted to work with dimensioned units, we would convert them to dimensionless ones using the two identities (4) and (5) and work with them in the numerical and analytical solution.

$$x = \frac{x^*}{L} \quad (4)$$

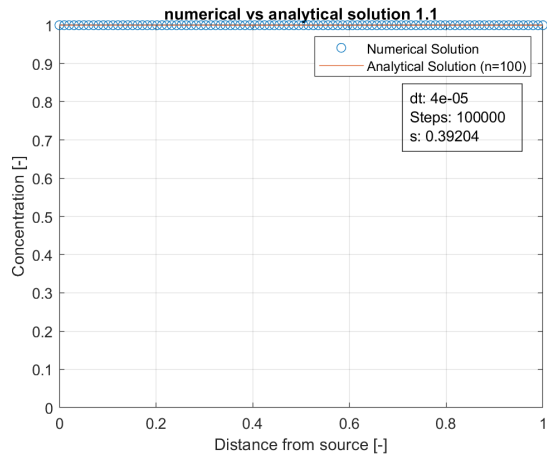
$$t = \frac{t^* D}{L^2} \quad (5)$$



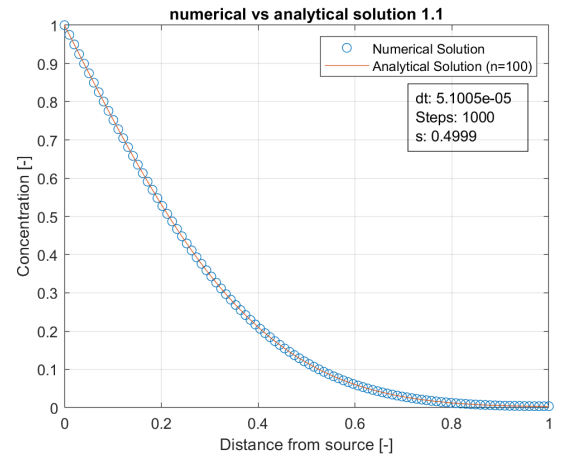
(a)



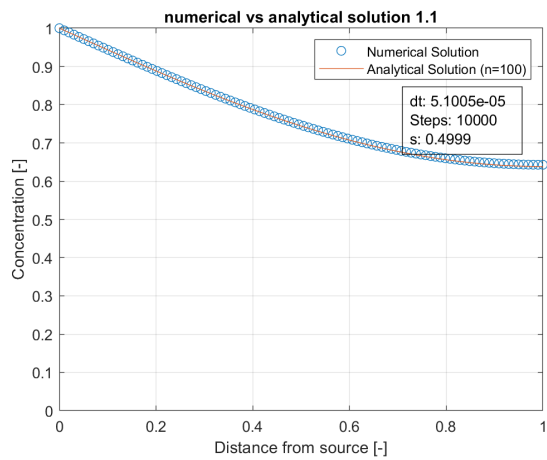
(b)



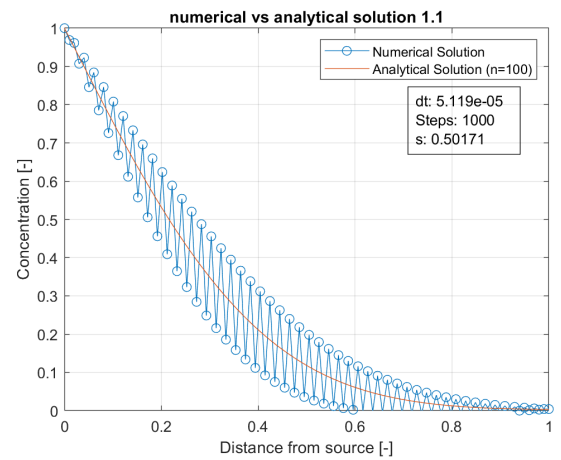
(c)



(d)



(e)



(f)

Figure 2: Numerical vs analytical solution for different step lengths and points in time

2 Exercise 1.2

The only difference between Exercise 1.2 and 1.1 is the homogenous Dirichlet boundary condition at $x = h$. The update procedure works as described above for Exercise 1.1, except for the concentration at $x = h$, where C_{end}^{n+1} is kept equal to $C_{end}^n = 0$.

The long term behaviour of the concentration results in a linear distribution from $x = 0$ to $x = h$ which makes sense because "particles" that enter the system at the source can now leave the system at $x = h$. This behaviour is particularly illustrative when compared to our results for Exercise 1.1. There the flux $\frac{\delta C}{\delta x}$ at $x = h$ was set to 0, which means every "particle" that enters into our system at the source, which is constant and set to 1, stays in the system. The concentration therefore eventually rises to 1 everywhere, given enough time (equilibrium concentration, see 3(d)). In contrast, the equilibrium in Exercise 1.2 is reached once the concentration decreases linearly from left to right as in 3(c).

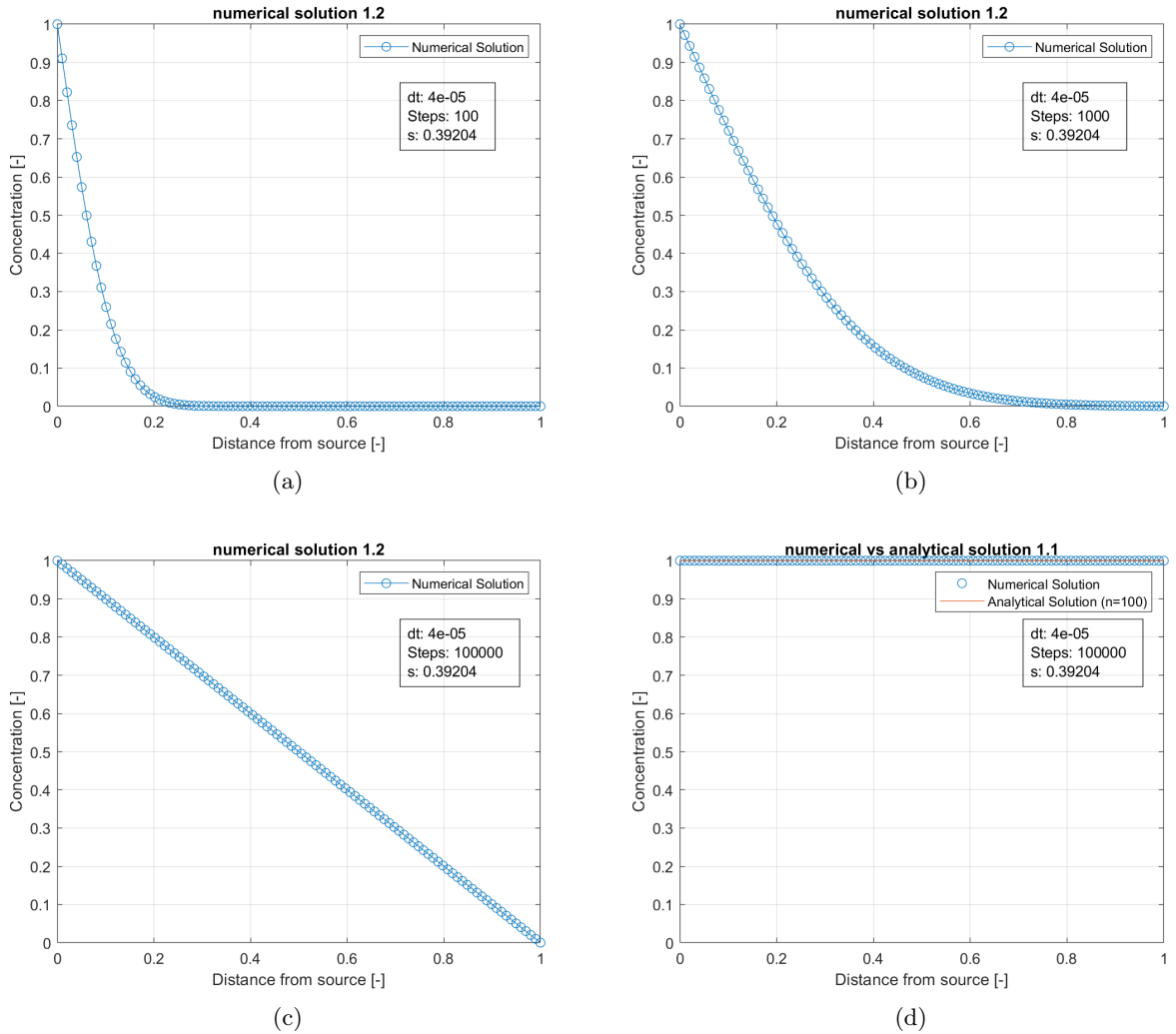


Figure 3: Two snapshots of the concentration in Exercise 1.2 at different time step (a-b). Comparison between long term behaviour of solution 1.2 (c) and solution 1.1 (d)

3 Exercise 1.3

In Exercise 1.3 we use the following implicit scheme that is 2nd order accurate in space and 1st order accurate in time:

$$C_i^n = -s \cdot C_{i-1}^{n+1} + (1 + 2s) \cdot C_i^{n+1} - s \cdot C_{i+1}^{n+1} \quad (6)$$

This leads to a linear system of equations with a tridiagonal matrix M. Again we have to incorporate the boundary conditions at $x = 0$ and $x = h$. For the Neumann boundary condition we take our findings from equation 1 into account. Eventually the Matrix M ends up looking like this:

$$M = \begin{bmatrix} 1 & 0 & 0 & \dots & 0 \\ -s & 1 + 2s & -s & \ddots & \vdots \\ 0 & \ddots & \ddots & \ddots & 0 \\ \vdots & \ddots & -s & \ddots & -s \\ 0 & \dots & 0 & -2s & 1 + 2s \end{bmatrix}$$

We then let the simulation run for different values of s and note that the calculation is stable in every case as can be seen in figure 4.

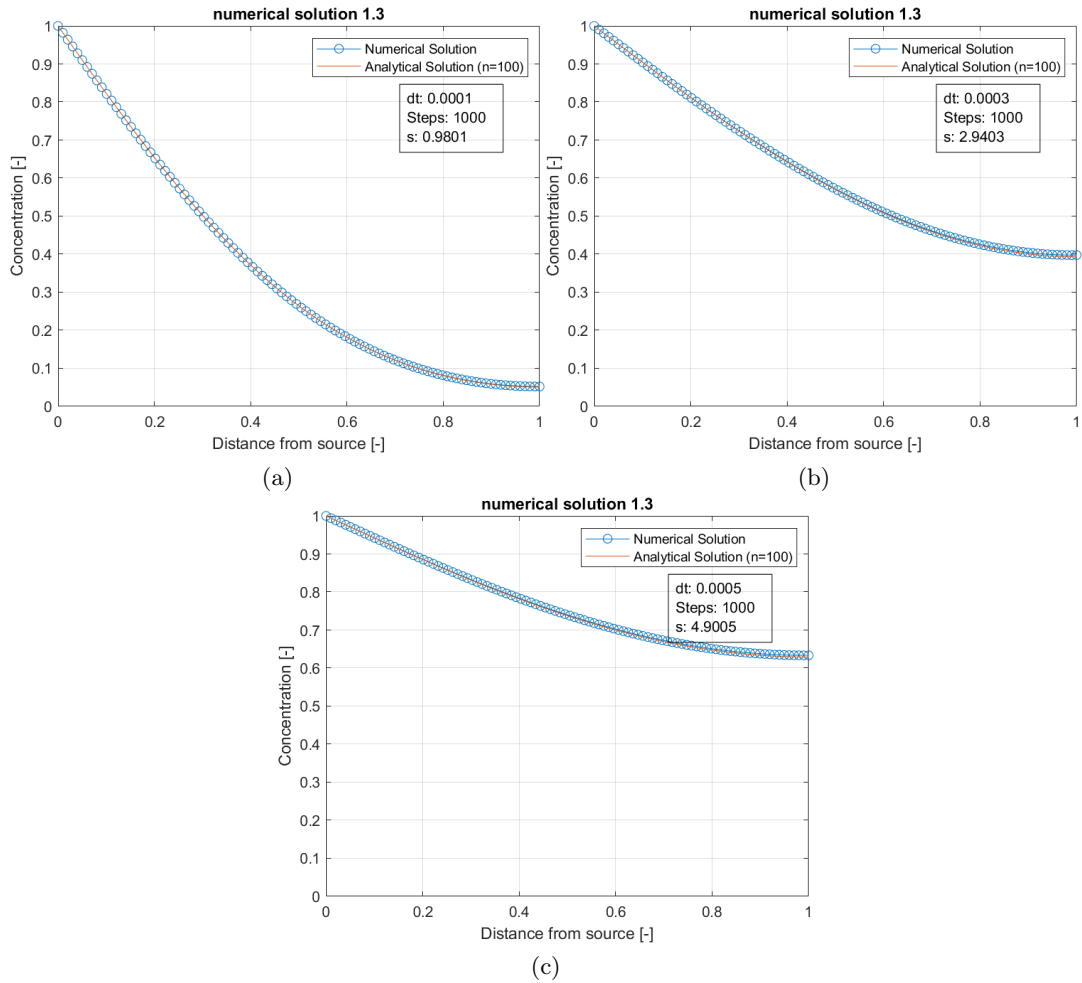


Figure 4: Numerical vs analytical solution for different step lengths and points in time

4 Exercise 1.4

For exercise 1.4 we use the so called Crank-Nicolson scheme that is 2nd order accurate in space and time:

$$-sC_{i-1}^{n+1} + 2(1+s)C_i^{n+1} - sC_{i+1}^{n+1} = sC_{i-1}^n + 2(1-s)C_i^n + sC_{i+1}^n \quad (7)$$

After incorporating the boundary conditions similar as in Exercise 1.3, we end up with the following matrix M for our system of linear equations:

$$M = \begin{bmatrix} 1 & 0 & 0 & \cdots & 0 \\ -s & 2+2s & -s & \ddots & \vdots \\ 0 & \ddots & \ddots & \ddots & 0 \\ \vdots & \ddots & -s & \ddots & -s \\ 0 & \cdots & 0 & -2s & 2+2s \end{bmatrix}$$

We then compare the solution in 1.3 with the solution in 1.4 for different settings and notice that the Crank-Nicolson scheme produces much less error than the implicit scheme from point 1.3.

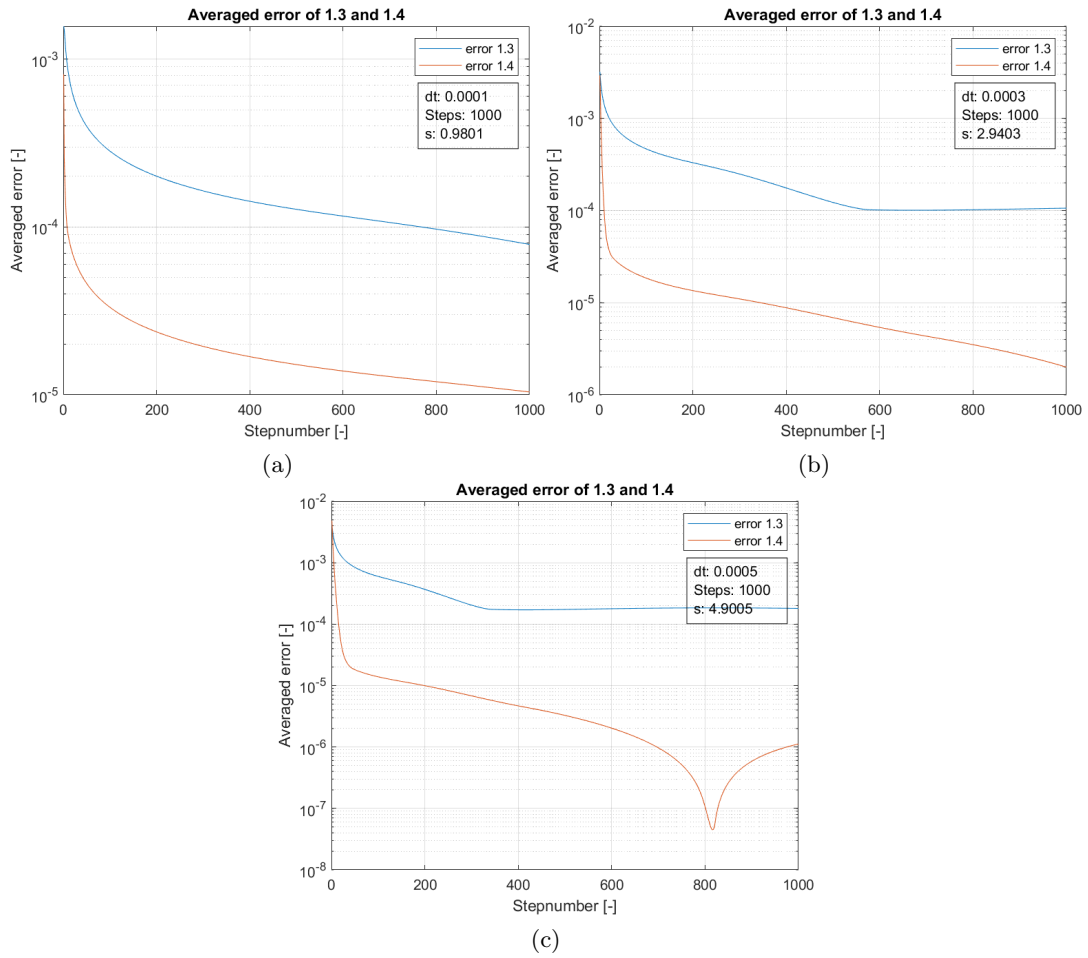


Figure 5: Comparison between the error in 1.3 and 1.4 for different settings

5 Exercise 2.1

To solve Exercise 2.1, we use the upwind scheme as given in the lecture:

$$C_i^{n+1} = C_i^n \cdot (1 - C_0) + C_0 \cdot C_{i-1}^n \quad (8) \quad C_0 = \frac{U \Delta t}{\Delta x} \quad (9)$$

Since there is no C_{-1} in (8), we calculate C_0^{n+1} using a forward instead of a backward approximation which results in the following identity:

$$C_0^{n+1} = C_0^n \cdot (1 + C_0) - C_0 \cdot C_1^n \quad (10)$$

We then look at the solution for varying Courant numbers C_0 . We start with $C_0 < 1$, shown in figure 6 and see that the smaller C_0 , the bigger the deviation from the analytical solution. That makes sense if we look at the term for the error ϵ :

$$\epsilon = \frac{U \cdot \Delta x}{2} \cdot (1 - C_0) \cdot \left[\frac{\delta^2 C}{\delta x^2} \right]_i^n \quad (11)$$

Nevertheless, the solution is stable as long as $C_0 \leq 1$.

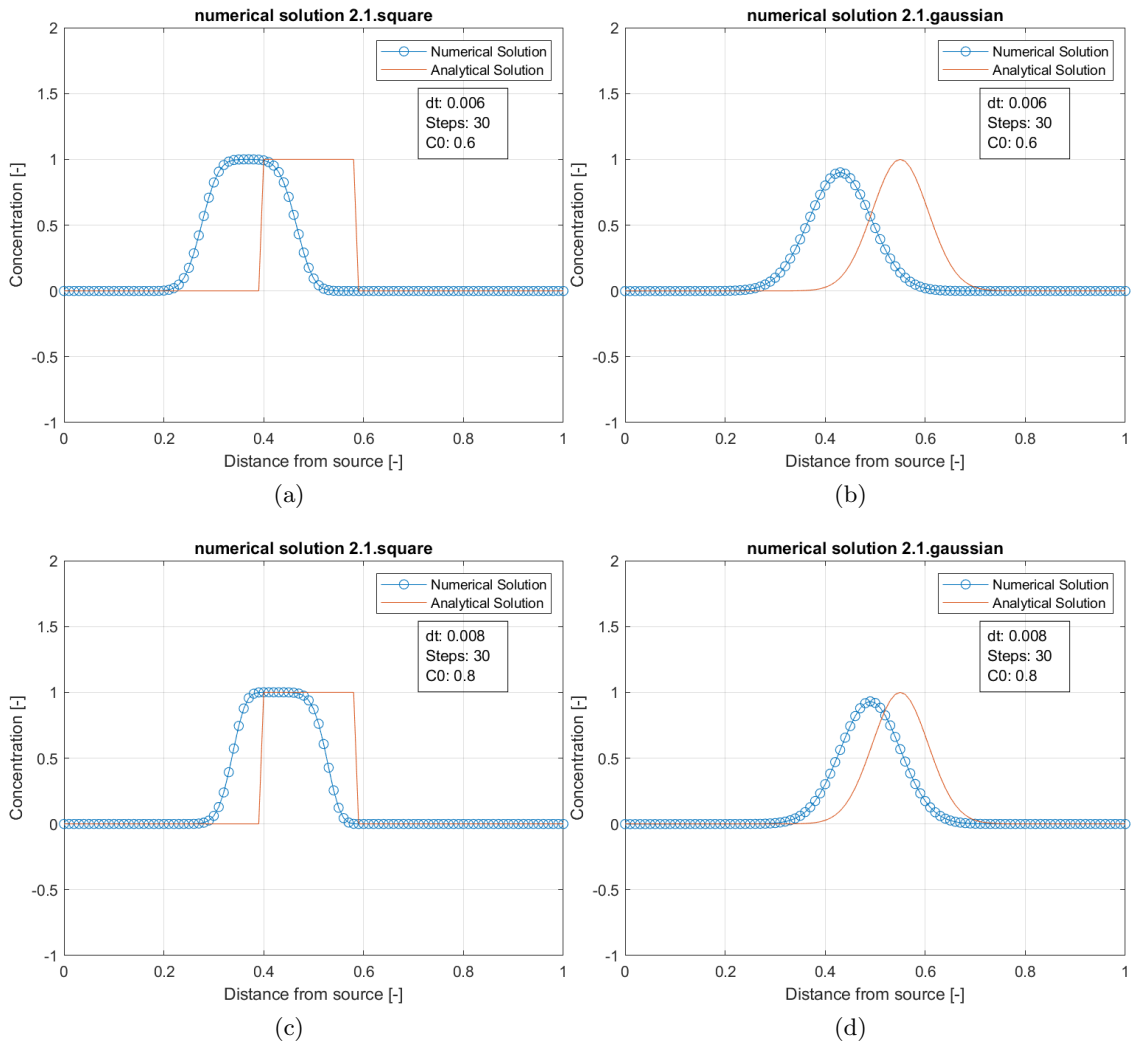


Figure 6: Numerical results for pure Advection for $C_0 < 1$

We then carry on with $C_0 = 1$ and see that the numerical error vanishes, see figure 7. For $C_0 = 1$, the first term in equation 8 vanishes and we are left with

$$C_i^{m+1} = C_0 \cdot C_{i-1}^m \quad (12)$$

which means the solution is simply drifting to the right with one step per iteration.

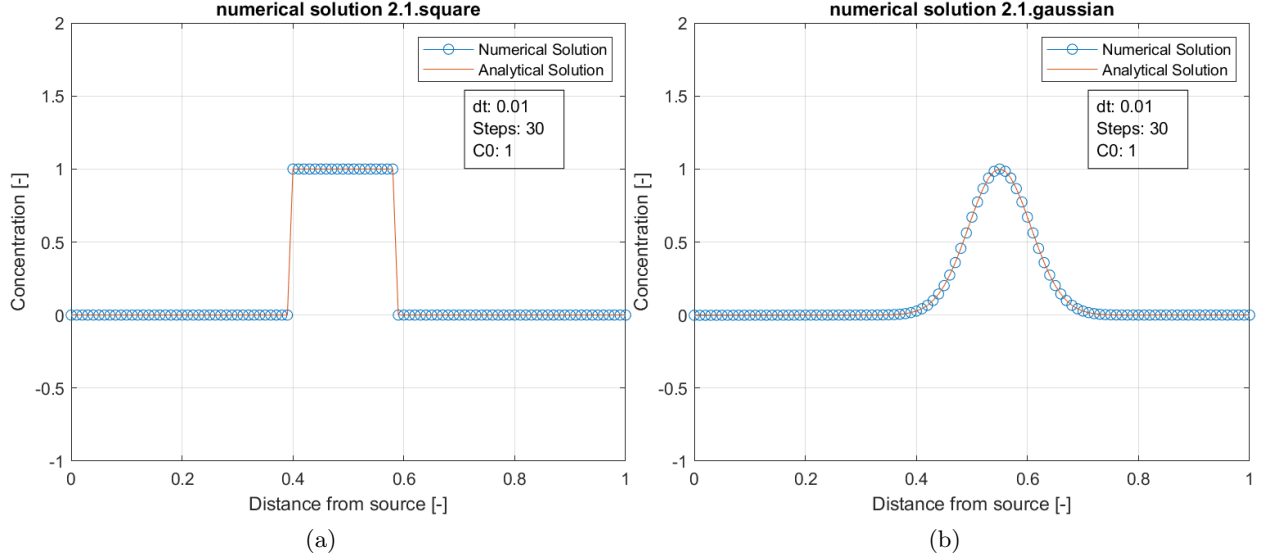


Figure 7: Numerical results for pure Advection for $C_0 = 1$

Finally, we look at the solution for $C_0 > 0$. In the case of the square pulse, the solution deteriorates very quickly. In case of the gaussian pulse, it takes some more steps until the effect gets visible but it is still there. This confirms the prediction, that the upwind scheme is only stable as long as $C_0 \leq 1$.

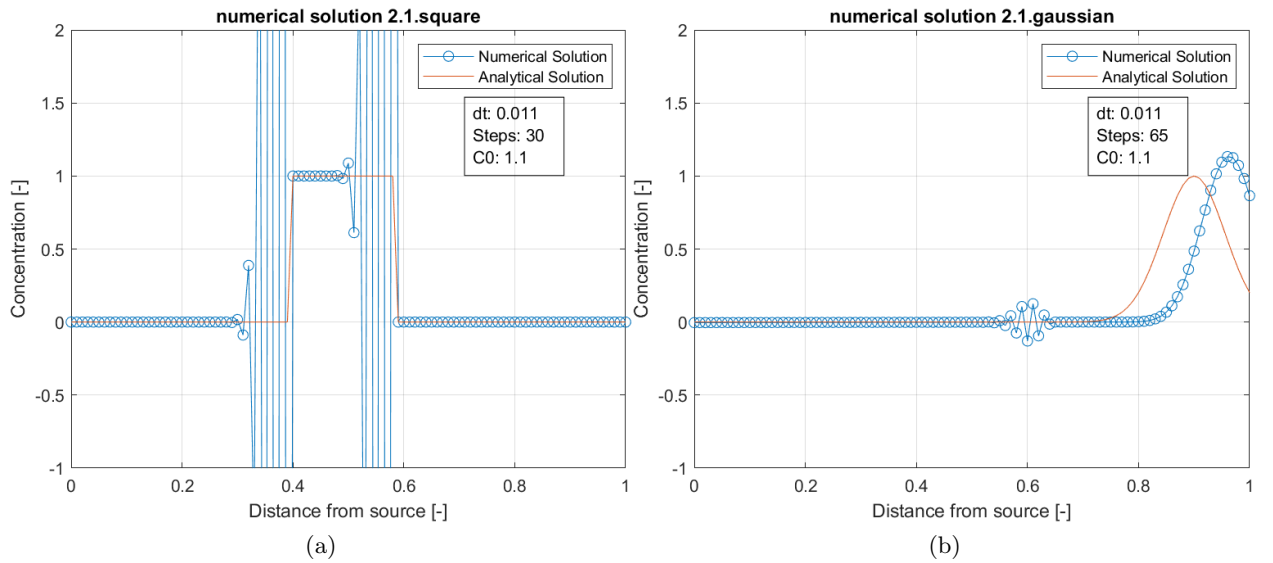


Figure 8: Numerical results for pure Advection for $C_0 > 1$